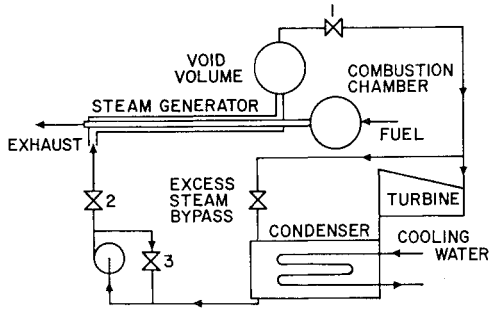

Fig. 2 Equipment schematic.

tubes will initially have some quantity of water present which will expand in addition to evaporating when heated. If the tubes are almost filled with water, a void expansion volume must be supplied as shown in Fig. 2. The energy equations are written as time derivatives and then are placed in finite difference form for computer solution. Polynomials are used to fit the steam table data necessary for the solution. A plot of the complete time transients are shown on the graph in Fig. 3.

The final starting transient is the time from the start of steam flow until the steam reaches its proper superheat temperature. Two conditions were evaluated for the final starting transient, but the case of initially full tubes is the only one of practical significance. The amount of superheating will be proportional to the surface in contact with the vapor. Energy equations for this case are placed in finite-difference form and solved by iteration techniques on a digital computer. The results of these calculations are shown in Fig. 4.

The liquid volume expands during the initial transient, and this puts excess water in the void space at the start of the final transient for initially full tubes. It will take 6 sec to evaporate this water before superheating starts. A summary of the results is given in Table 2.

The size of the generator can be reduced if the average gas temperature is increased by increasing the gas flow rate, but it would increase the initial mass of fuel carried by 120 lb for each minute of operation.

The time variations in the different cases for the initial transient are primarily due to variations in the amount of heat-transfer surface in contact with the liquid, as increased contact area increases the evaporation rate. The temperature rise in the final transient for the tubes initially filled with water is very slow at first because of the small surface initially exposed to the dry steam. The steam generation rate is initially higher than required, and the steam bypass valve must open to maintain pressure. This situation disappears as steady state is approached due to a decreasing amount of liquid in contact with the surface.

The total transient is less than 1 min, and it takes about 20 sec for operation to begin. This may appear short, but

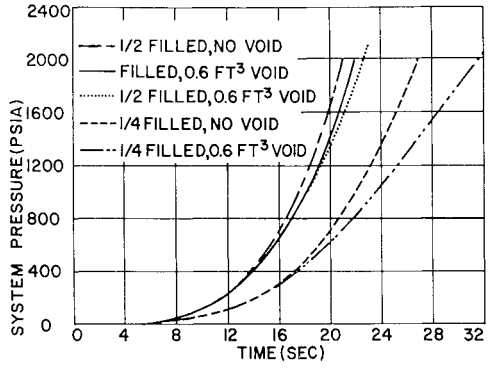

Fig. 3 Initial starting transient.

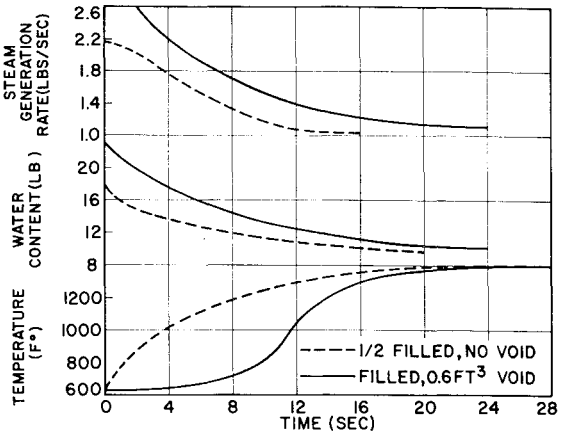

Fig. 4 Final starting transient.

some applications would require auxiliary power during the initial transient. The case of tubes $\frac{1}{2}$ full with no excess void represents the shortest total transient, but there would be considerable danger of tube burnout during the initial transient if they were not completely filled with water. The tube length can be shortened by using higher gas flow rates and gas exhaust temperatures. This, however, will require more fuel to be carried plus reduce the heat-transfer resistance on the gas side, which will raise tube wall temperature and weaken the material.

Reference

[1] Rounthwaite, C. and Clouston, M., "Heat transfer during evaporation of high quality water-steam mixtures flowing in horizontal tubes," *Modern Developments in Heat Transfer* (American Society of Mechanical Engineers, New York, 1961), Part I, pp. 200–211.

High-Temperature Inorganic Adhesives for Electromagnetic Applications

F. A. Barr* and T. S. Montgomery†
Whittaker Corporation, San Diego, Calif.

THE mission requirements and performance characteristics of current and advanced aerospace vehicles and weapons systems are continually demanding more refined and efficient detection and ranging equipment. The radomes that contain such electromagnetic devices must compromise the performance of this equipment as little as possible while still offering aerodynamic smoothness and environmental protection. Only ceramic materials, with their high-temperature stability, resistance to rain erosion, and uniform electrical properties, are presently available for the fabrication of such radomes. Unfortunately, producing a monolithic ceramic radome in the sizes and configurations required for optimum vehicle performance has proved to be difficult and sometimes impossible. Processing equipment and techniques,

Presented as Preprint 64-355 at the 1st AIAA Annual Meeting, Washington, D. C., June 29–July 2, 1964; revision received August 31, 1964. This work was supported in part by the U. S. Air Force through the Chemical Processing Branch, Manufacturing Technology Division, Air Force Materials Laboratory, Wright-Patterson Air Force Base, Ohio.

* Research Specialist, Ceramics, Refractories Research Department, Narmco Research and Development Division.

† Senior Research Ceramist, Refractories Research Department, Narmco Research and Development Division.

Table 1 Properties of 97.6% radome grade alumina

Property	Published[a]		Narmco[b]	
Temperature, °F	75	1000	75	1000
Strengths, 1000 psi				
Tensile	30	...	26	15
Compressive	300	...	250	215
Flexural	46	...	29	25
Elastic modulus, 10^6 psi	45	...	...	...
Dielectric constant, 9.375 Gc	9.0	9.5	8.26	8.8
Loss tangent $\times 10^{-4}$, 9.375 Gc	5	7	6	0
Shear modulus, 10^6 psi	22	21	...	...
Poisson's ratio	0.21	0.19	...	...
Density, lb/in.^{3}	0.035		...	
Thermal conductivity, Btu/hr-ft^3-°F/ft	10.7		...	
Thermal expansion, in./in.-°F (75 to 1000°F)	4.0×10^{-6}		3.9×10^{-6}	

[a] Based on manufacturer's literature.
[b] Results obtained by Narmco Research and Development.

particularly press capacity and firing shrinkage control, places limits on the maximum size of a ceramic radome produced by present technology.

One method for fabricating large, structurally and electrically-acceptable radomes involves bonding together available, low-dielectric, ceramic "tiles" using mosaic techniques.[1] The result of a manufacturing methods development program suggested the mosaic approach to be feasible for producing ogival radomes. Curved tiles approximately 4 in.[2] would be bonded and fabricated into a radome shape nearly 9 ft high with a 3-ft diam. The goals of the program required a combination of structural, thermal, and electrical properties for both the ceramic segments and adhesive binder employed. Ceramic segment bodies of the refractory oxides of alumina, beryllia, and zirconia were investigated. Tests included flexure, compression, tension, and electromagnetic properties both at room and elevated temperatures.

The structural and electrical requirements of the mosaic-type radome dictated that the selected adhesive be capable of operating at temperatures of 1000°F, while being compatible and not appreciably changing the dielectric constant and loss tangent of the base alumina at a frequency of 9.375 Gc (gigacycles). Compatibility implied good wetting of the alumina by the adhesive, as well as similar thermal expansion characteristics. The minimum bond strength required for structural loads was calculated to be 4000 psi in shear strength for composite lap joints. The inorganic adhesives were prepared as fine mesh powders and were applied to the alumina segments by spraying, dipping, or painting, using a nitrocellulose vehicle.

Discussion of Results

The ceramic segments investigated were calcia-stabilized zirconia, sintered and hot-pressed beryllia, and several grades of high-purity alumina (96–99.5% Al_2O_3). The calcia-stabilized zirconia appeared inadequate because of poor electrical and structural properties. Beryllia was eliminated on the basis that it was roughly equivalent to alumina, and considering all factors, the added handling hazards could not economically justify the selection of beryllium oxide. Evaluation of the high-alumina bodies (96–99.5%) indicated that a nominal purity of 97.6% was satisfactory from the standpoint of over-all performance. Therefore, all selected candidate adhesives were evaluated for their compatibility and composite properties with this alumina. Table 1 lists the general properties of the selected alumina material.

The investigation was conducted primarily on inorganic, "high-temperature" adhesives that had previously been used successfully in bonding either ceramic powders, glass shapes or ceramic foam materials.[2–5] These included room- or low-temperature setting ceramic cements, which, although stable to high temperatures, had low mechanical strength. The three most promising types prior to the development of the actual selected adhesive were 1) thermal-setting devitrified sealing glass, 2) ceramic eutectic of refractory oxide and metal pyrophosphate, and 3) aluminosilicate glass. However, these adhesives (see Table 2) did not meet the specified goals of the program. The first had a relatively low curing temperature, thus offering a low fabrication temperature with relatively simple tooling problems. However, its thermal expansion mismatch with alumina could greatly manifest itself when a radome size of 9 ft is contemplated, and the inability to form tensile specimens caused concern. The crystalline eutectic (item 2) did not possess adequate mechanical strength (average shear strengths of only 3360 psi were obtained), and its low

Table 2 Physical and electromagnetic properties of candidate ceramic adhesives

Property	Devitrified sealing glass		Ceramic eutectic		Aluminosilicate glass		Modified aluminosilicate glass	
Temperature, °F	75	1000	75	1000	75	1000	75	1000
Joint lap shear strength, psi	4450	4280	3360	3360[b]	4570	4130	11,200	10,000
Solid compressive strength, psi	45,000	...	...	...	48,000	...	49,000	...
Joint tensile strength, psi	...[a]	...	...	...	4000	...	10,400	...
Joint flexural strength, psi	22,600	...	...	...	22,000	...	21,500	...
Dielectric constant, 9.375 Gc								
Solid body	5.23	5.57	6.10	6.12	5.47	6.73	5.86	6.79
Composite joint (Al_2O_3)	8.25	8.71	...	...	8.38	8.88	8.26	8.70
Loss tangent, 9.375 Gc								
Solid body	0.0039	0.0033	0.0049	0.0079	0.0212	0.1328	0.0154	0.0815
Composite joint (Al_2O_3)	0.0005	0.0015	...	...	0.0009	0.0034	0.0009	0.0032
Chemical attack, % wt loss, 24 hr								
10% Sodium hydroxide	3.6		0.7		0.03		0.05	
10% Hydrofluoric acid	24.6		16.0		21.3		24.0	
10% Aqua regia	8.3		10.0		0.03		0.04	
Thermal expansion, in./in./°F								
75 to 1000°F	2.2×10^{-6}		2.1×10^{-6}		4.4×10^{-6}		3.6×10^{-6}	
Environmental effect								
Boiling water, 24 hr	None		None		None		None	
Fungus (MIL E-5272C)	None		None		None		None	
Firing temp, °F	1382 ± 50		1910		2250		2150	

[a] Unable to make satisfactory specimen.
[b] Test specimens susceptible to thermal shock.

thermal expansion caused failure in the bondline upon thermal cycling. Its other properties were satisfactory, particularly the dielectric constant and loss tangent, which were quite uniform over the temperature range to 1200°F. The aluminosilicate glass (item 3) had a mechanical strength similar to item 1, and desirable thermal expansion value compared with 4.0 × 10^{-6}in./in.-°F known for the 97.6% Al_2O_3. Although monolithic solid test specimens of the aluminosilicate glass were inferior in electrical properties, its presence as a thin bondline in composite specimens was completely acceptable. However, the severe requirements of the program dictated that an improved adhesive be developed.

A significant increase in shear strength was obtained with a modified aluminosilicate glass, which has good wetting and compatibility with the alumina segments and develops outstanding mechanical strength when cured at temperatures of near 2150°F. Its physical and electromagnetic properties are listed in Table 2. Numerous lap shear joint specimens had average shear strengths of 10,000 psi at room temperature and at 1000°F. Joint tensile strengths also were much higher than any of the previously mentioned adhesives, with an average value of 10,400 at room temperature; the range for the lap shear specimens was from 8000–13,000 psi. However, specimen preparation and testing method contributed to range of shear strengths observed. The majority of the shear-strength values concentrated around the obtained average indicated that this should be a reasonable value to use for screening purposes.

The main cause of concern in using an adhesive of this type was the effect it would have on the dielectric constant and loss tangent of the composite structure. By nature of its chemical formulation, this type of glass was known to have high electrical losses. This was confirmed when solid samples of the aluminosilicate glass adhesives were tested for their dielectric constant and loss tangent at 9.375 Gc. The general technique employed for forming test samples of the adhesives for mechanical, thermal, and electromagnetic tests was to fuse samples in graphite molds. The solid test specimens were prepared by pressing the fine mesh powder at 10,000 psi and heating in graphite molds to approximately 2250°F. After heating, the samples had vitrified to a dense state simulating their physical state in composite bondlines. Test samples 0.330 × 0.390 × 0.890 ± 0.001 in. were machined from the monolithic, solid bodies and measured for dielectric constant and loss tangent by the shorted waveguide method.‡ As expected, the test results showed solid samples of the modified aluminosilicate adhesive to have high loss tangents as follows: room temperature, 0.0154; 1000°F, 0.0815; and 1200°F, 0.235. The dielectric constant, increased from 5.86 at room temperature to 6.93 at 1200° F.

The main objective was to determine the effect of a relatively high loss tangent material in the bondline on the overall property of the composite structure. Specimens were prepared to simulate the bondline position in actual radome use. Specimens (0.330 × 0.390 × 0.890 in.) were machined containing bondlines measuring 5 to 7 mils. These were measured for loss tangent and dielectric constant both perpendicular and parallel to the bondline at 9.375 Gc. Figure 1 shows the respective dielectric constant and loss tangent curves for the composite structures and for the 97.6% alumina reference material.

The electromagnetic values obtained for the composite specimen containing the modified aluminosilicate adhesive were similar to the base alumina material. When tested perpendicular to the bondline, a dielectric constant of 8.26 was obtained for the composite compared to 8.24 for the base alumina sample. At 1200°F, the dielectric constant had only increased to 8.81 and compared favorably to the 8.82 value recorded for the 97.6% alumina. The loss tangent perpendicular to the bondline at room temperature was 0.0009

‡ Conducted at Melpar, Inc.

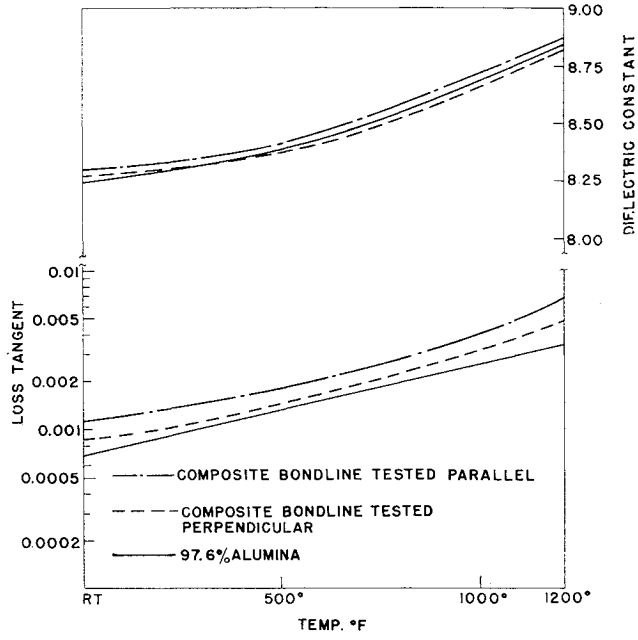

Fig. 1 Loss tangent and dielectric constant at 9.375 Gc; composite samples containing modified aluminosilicate adhesive.

compared to 0.0007 for the base alumina. The composite tested normal to the bondline was only slightly higher than the base alumina, measuring 0.0048, as compared to 0.0035 at 1200°F. Thus, when the modified aluminosilicate adhesive was employed in thin bondline to bond alumina segments, it showed no adverse effect. The resulting electromagnetic properties were essentially those of the segment material per se.

Summary

The modified aluminosilicate adhesive offers structural advantages when compared to the thermal setting, devitrified sealing glass, and the aluminosilicate glass. The crystalline ceramic eutectic material did not have lap shear strength sufficient for the discussed radome application.

The simplest comparison involves the modified magnesium aluminosilicate and the aluminosilicate glass-type adhesives, as they are relatively similar in composition and physical properties. The superior lap shear and joint tensile strength as well as the slightly lower thermal expansion coefficient favors the use of the modified aluminosilicate adhesive. Differences in other properties are relatively insignificant.

A comparison of the devitrified sealing glass-adhesive with the modified aluminosilicate glass-type adhesive encompasses an application problem. These adhesives are of differing types, having a wide difference in firing temperatures and exhibiting different thermal expansion characteristics. Again, the modified aluminosilicate type exhibits superior structural capabilities, and its dielectric constant and loss tangent in a joint are both acceptable. The adhesives per se are quite different electrically with the devitrified sealing glass having a definite superiority. However, as previously mentioned, this would only be important when very thick and thus unacceptable joints are considered. The thermal expansion mismatch existing between the alumina and the devitrified sealing glass may be critical when large, surface-contact areas are considered.

Electromagnetic testing of the composites containing the aluminosilicate adhesives showed that similar dielectric constant values were obtained for specimens tested parallel to the bondline, whereas higher loss tangent values were obtained when tested parallel to the bondline, indicating the possibility of a definite maximum bondline thickness at which

the loss tangent might become detrimental. The bondline thickness in radome fabrication would not be any greater than the 5- –7-mil bondline employed in the composite tests specimens. Since the loss tangent values obtained for all composite samples were well within the target goals of 0.005 at room temperature and 0.010 at 1000°F, it is believed that this would not be a problem in radome construction.

The curing temperature of each adhesive is simultaneously advantageous and limiting. The devitrified sealing glass, firing at 1382°F, offers a low fabricating temperature for the radome size considered in this paper with relatively simple tooling problems. The modified aluminosilicate adhesive, curing at 2150°F, requires a substantially longer firing cycle, and tooling problems would be more formidable. However, low-temperature tooling techniques would be a limiting factor in advancing the "state of the art" temperature-wise for future radomes.

References

[1] Filippi, F. J., "Composite ceramic radome manufacture by mosaic techniques," Contract AF 33(657)-10111, Interim Engineering Progress Rept, IR-7 984, Vols. II and III (1963).

[2] Cornely, K. W., "New cements prove suitable for applications above 4000°F," Ceramic Age **78**, no. 1, 52–53 (1962).

[3] Reeder, R. and Long, R. A., "Ceramic crystalline binders for refractory oxides," American Ceramic Society, Paper 4-M-62 (1962).

[4] Claypole, S. A., "Composite article and method," U. S. Patent No. 2,889,952 (June 9, 1962).

[5] Caldwell, O. G., "The development of high purity alumina laminates with specific dielectric constants," Gladding McBean and Co., Contract NOas 59-622c (January 1961).

Weight Considerations in the Storage of Secondary Energy

WILLIAM J. WACHTLER*
New Mexico State University, University Park, N. Mex.

Nomenclature

L = cylindrical length, in.
P = internal chamber pressure, psi
r = radius, in. (see Fig. 3)
R = radius, in.
t = wall thickness, in.
W = storage weight, lb
α = angle, degrees (see Fig. 3)
η = volumetric loading efficiency, dimensionless
ξ = geometric ratio, dimensionless
σ = allowable stress, psi
σ_h = hoop stress, psi
σ_m = meridional stress, psi
ρ = material density, lb/in.[3]

Subscripts

p = primary
s = secondary

Introduction

THE propellant supply from the missile tanks in a liquid propulsion system or the generated high-pressure gas from the motor chamber in a solid propulsion system is often used for other purposes in addition to producing thrust. In a liquid system, a small portion of the propellant is often burned in a separate gas generator or bled off from the combustion chamber and used to drive turbopumps and other auxiliary systems. In the case of solid propulsion systems, designers have considered hot gas bled off from the combustion chamber for thrust vector control. With the continuing need for weight conservation in missile design to optimize performance, weight comparisons must be made before finalizing designs. Therefore, when the designer considers utilizing primary storage for secondary use, it will serve him well to investigate the weight tradeoff. This note points out the major parameters that affect weight tradeoffs for the more common geometric configurations that may be used as a secondary energy storage vessels.

Received July 17, 1964.

* Project Engineer, Physical Science Laboratory (Rocket Systems).

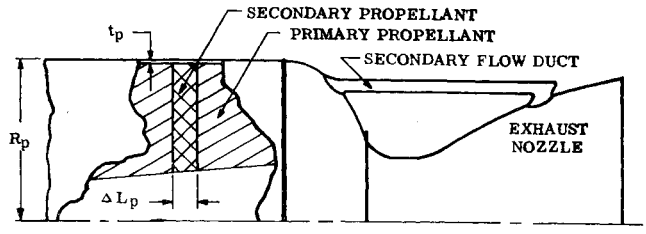

Fig. 1 Primary storage configuration.

Analysis

Consider the solid propellant motor (Fig. 1) in which additional primary storage volume is provided for secondary propellant. This additional secondary propellant is used to generate a secondary flow that is injected into the primary gas stream near the nozzle exit for thrust vector control. It is assumed that the additional secondary propellant volume is occupied by the cylindrical portion of this primary system and that the additional propellant surface area required for the generation of secondary flow is obtained by lengthening the motor by (ΔL_p).

Two secondary storage vessel configurations (Figs. 2 and 3) are considered in this analysis as replacements for the additional primary storage volume required in this primary configuration. First considering the cylindrical hemispherical configuration (Fig. 2) the stresses developed are[1]

$$\sigma_h = PR/t \qquad \sigma_m = PR/2t \tag{1}$$

and the additional primary storage weight (ΔW_p) and the secondary storage weight (W_s) are given by

$$\Delta W_p = 2\pi\rho_p R_p^2 P_p \Delta L_p/\sigma_p \tag{2}$$

$$W_s = 2\pi\rho_s R_s^2 P_s (L_s + R_s)/\sigma_s \tag{3}$$

Since equal storage volumes are required,

$$\Delta L_p = \frac{\eta_s}{\eta_p}\frac{R_s^2}{R_p^2}\left[L_s + \frac{4}{3}R_s\right] \tag{4}$$

Upon substitution of (4) in (2) and dividing by (3), the tradeoff becomes

$$\Delta W_p/W_s = \beta(\xi + \tfrac{2}{3})/(\xi + \tfrac{1}{2}) \tag{5}$$

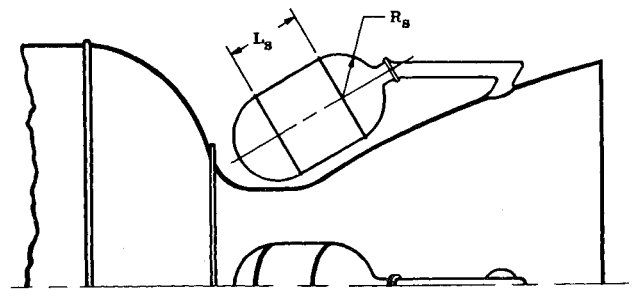

Fig. 2 Secondary storage cylindrical hemispherical configuration.